2 Metallic point contacts as a physical tool

Already more than 100 years ago Drude developed a theory for the electrical and thermal conduction of metals based on the classic kinetic theory of gases. Drude considered a metal to be a lattice-reservoir filled by a gas of electrons, which move freely between the scattering events on the ions of the lattice. Considerable improvements in the quantitative estimates were made later by Sommerfeld, which account for the quantum mechanical Pauli exclusion principle of the electrons, what leads to the Fermi–Dirac energy distribution of the electrons with occupied electron states up to the Fermi energy. At zero temperature, the Fermi surface separates in wave vector **k**-space the occupied electronic states from the empty ones. For free electrons, the Fermi surface consists of a sphere with radius k_{F}. In real crystalline metals, the shape of the Fermi surface is much more complicated and determined by the number of conduction electrons per atom as well as the symmetry of the lattice. Because the electron states close to the Fermi surface are responsible for the main characteristic properties of metals, *viz.* electrical and thermal conductivity, superconductivity, thermoelectric effect, and so on, knowledge of the Fermi surface has an important meaning for the understanding of the electronic transport. Many experimental methods exist for the investigation of the Fermi surface. The most important ones are known as the de Haas–van Alphen and the Shubnikov–de Haas effects, where oscillations of thermodynamic and transport properties of metals in a magnetic field are measured to get detailed information on the shape of the Fermi surface. In this chapter, we briefly describe milestone experiments connected with the main topic of this book. These achievements gave undoubtedly the necessary impact to the further development of point-contact spectroscopy.

2.1 Electron focusing

Sharvin (1965) theoretically examined for the first time the resistance of a *ballistic* contact where the mean free path l of the electrons is larger than the size d of the constriction. Here one can model the contact as a circular orifice of diameter d in an insulating plane between two metallic parts (Fig. 2.1). Sharvin's description of the contact resistance was as follows. In the voltage-biased ballistic contact, the speed increment δv for an electron

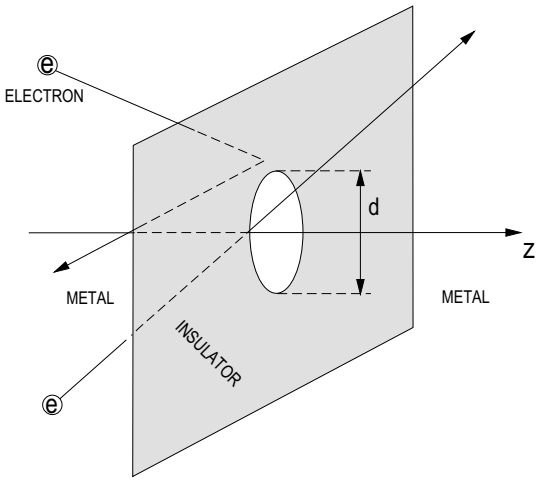

Fig. 2.1. Model of a ballistic point contact presents an orifice with diameter d in an insulating plane between two metallic banks along with trajectories of electrons.

passing the orifice is proportional to the applied voltage: $\delta v = eV/p_{\mathrm{F}}$, where p_{F} is the Fermi momentum. This results in a current I through the contact: $I \simeq e(\pi\, d^2/4)\, n\, \delta v = (\pi\, d^2/4)\, (n\, e^2/p_{\mathrm{F}})\, V$, where n is the electron density. Using the Drude formula for the resistivity $\rho = p_{\mathrm{F}}/ne^2 l$, one finds an expression for the resistance of a contact: $R \simeq 4\rho l/\pi d^2$. The integration over all possible angles gives a numerical factor 4/3 leading to the Sharvin resistance of a circular contact:

$$R_{\mathrm{Sh}} = \frac{16\rho l}{3\pi d^2}. \tag{2.1}$$

The Sharvin resistance depends only on the contact dimension d and is independent of the material purity, whereas $\rho l = p_{\mathrm{F}}/ne^2$ is a material constant for a specific metal. It is of interest to compare the ballistic resistance with the resistance of a contact in the opposite limit $d \gg l$. Already Maxwell (1904) has calculated the resistance of a "dirty" metallic contact and found that it depends on the resistivity and the contact diameter in a simple way:

$$R_{\mathrm{M}} = \frac{\rho}{d}. \tag{2.2}$$

Apart from a geometrical constant, this expression can be easily deduced by considering the resistance of a sample of length d and diameter d.

Realizing the mechanism of ballistic electrical transport in small metallic constrictions at low temperatures, Sharvin proposed to use contacts placed on the opposite sides of a thin metallic slab for a study of the Fermi surface. One of them is used as an injector of electrons and the other as a detector of electrons. By applying the appropriate longitudinal magnetic field, injected electrons can be focused onto the opposite electrode [see Fig. 2.2(a)]. The

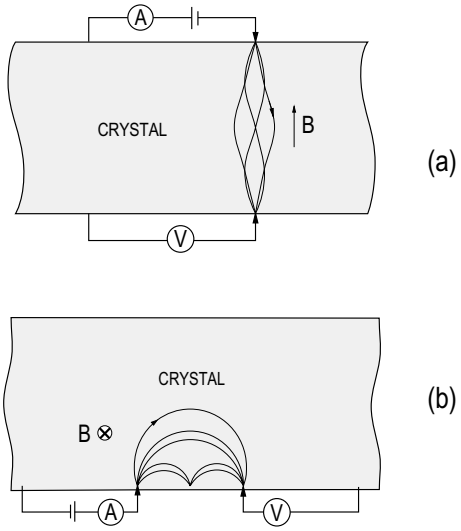

Fig. 2.2. (a) Longitudinal electron focusing in a magnetic field according to Sharvin (1965). (b) Transverse electron focusing in a magnetic field according to Tsoi (1974).

idea is based on the ballistic electron flow without collisions between the two contacts. In this case, the trajectory of the electrons in a magnetic field is determined by the geometry of the Fermi surface. Deflected by a magnetic field of appropriate focusing strength, the injected electrons cause an increased concentration of charge carriers and therefore an increased potential at the second contact. In the experiments of Sharvin, it is not necessary that the flow of electrons through the contact be ballistic or energy conserving; only the trajectory between the contact periphery of injection and detector contacts should behave ballistically without collisions. Collisions between emitter and collector would strongly decrease the amount of focused electrons.

In 1974, Tsoi further developed Sharvin's method of focusing by placing the emitter and collector contacts on the same side of the metallic slab and applying a transverse magnetic field parallel to the surface [Fig. 2.2(b)]. This method was found to be simpler compared with the Sharvin one, where it was difficult to place two contacts exactly opposite to each other on a thin metal slab. For increasing magnetic field, or decreasing cyclotron radius, the direct focusing of electrons is followed by electron focusing after specular reflection from the inside of the metal surface. In Fig. 2.2(b), we have shown electron trajectories close to the field for direct focusing and for focusing after one internal reflection. Transverse focusing provides not only information on the Fermi surface, but also the probability of specular reflection from the crystal surface. Moreover, other scattering boundaries such as the normal metal-superconductor interface can be investigated. These examples already show that metallic point contacts are a powerful tool in transport experi-

ments where the *ballistic* regime of electron transport with minimal electron scattering plays a decisive role.

2.2 Normal-metal contacts

During the investigation of small constrictions between two metallic films separated by a thin (a few nanometers) dielectric layer, in the beginning of the 1970s, Yanson paid attention to their nonlinear current-voltage ($I - V$) characteristics at helium temperature. Further detailed study showed that these deviations from Ohm's law occurred at an energy eV corresponding to the phonon frequencies of the metals under study. Moreover, Yanson (1974) found that the measured second derivative $\mathrm{d}^2V/\mathrm{d}I^2(V)$ of the $I - V$ curve resembles the Eliashberg function $\alpha^2F(\omega)$ of the electron–phonon interaction. Roughly speaking, the dimensionless $\alpha^2F(\omega)$ function is the convoluted product of the phonon density of states $F(\omega)$ and the matrix element squared α^2 of the electron–phonon interaction. As shown in Fig. 2.3, the maxima of

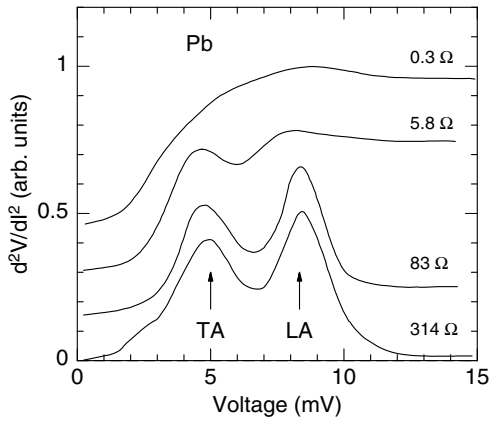

Fig. 2.3. Second derivative of $I - V$ curves for a Pb tunnel junction with microconstriction at helium temperature in the process of successive decreasing of the resistance of the constriction from 314 Ω (bottom curve) to 0.3 Ω (top curve). The positions of longitudinal acoustic (LA) and transverse acoustic (TA) phonon peaks in Pb are indicated by arrows. The curves are offset vertically for clarity. Data taken from Yanson (1974).

the $\mathrm{d}^2V/\mathrm{d}I^2(V)$ point-contact spectra for a Pb constriction coincide with the main phonon peaks of Pb – transverse and longitudinal. Why $\mathrm{d}^2V/\mathrm{d}I^2(V)$ directly reflects $\alpha^2\,F(\omega)$ is easily to see by including in the Sharvin formula for the contact resistance a contribution (2.2) caused by scattering of electrons in the constriction, such that

$$R \simeq \frac{16\rho l}{3\pi d^2} + \frac{\rho}{d}. \tag{2.3}$$

This expression of the contact resistance is an extrapolation between the two limiting expressions of a clean contact ($l > d$) and of a dirty contact ($l < d$) [see Eqs. (2.1) and (2.2)]. The second term of (2.3) describes the corrections to the ballistic Sharvin expression caused by scattering, which will be small in the limit $l > d$. We can rewrite (2.3) as an expansion in d/l

$$R \simeq R_{\mathrm{Sh}} \left(1 + \frac{3\pi d}{16\, l}\right) = R_{\mathrm{Sh}} \left(1 + \frac{3\pi d}{16 v_{\mathrm{F}} \tau}\right). \tag{2.4}$$

An energy-dependent scattering time $\tau(eV) = l(eV)/v_{\mathrm{F}}$ leads to a voltage-dependent contact resistance $R(V)$. Using a golden rule argument for the emission of phonons by a nonequilibrium electron at an energy eV above the Fermi energy, $\tau_{\mathrm{el-ph}}(eV)$ can be related to the electron–phonon interaction function $\alpha^2 F(\epsilon)$, according to Grimvall (1981),

$$\tau^{-1}_{\mathrm{el-ph}}(eV) = \frac{2\pi}{\hbar} \int_0^{eV} \alpha^2(\epsilon) F(\epsilon)\, \mathrm{d}\epsilon. \tag{2.5}$$

Then the derivative of (2.4) yields

$$\frac{\mathrm{d}R}{\mathrm{d}V} \left(\propto \frac{\mathrm{d}^2 V}{\mathrm{d}I^2}\right) \simeq R_{\mathrm{Sh}} \frac{3\pi^2\, ed}{8\hbar v_{\mathrm{F}}} \alpha^2 F(eV). \tag{2.6}$$

This estimation shows directly the proportionality between the second derivative of the $I-V$ curves measured by Yanson (1974) and the electron–phonon interaction function. Using a picture of ballistic electron trajectories, electrons passing through the constriction gain the excess energy eV and can relax by the spontaneous emission of phonons with maximum energy eV. Some of the electrons are reflected back from the contact because of these electron–phonon scattering processes, leading to a backflow correction to the current through the contact. Finally, this results in an $I - V$ characteristic with nonlinearities at voltages corresponding to the characteristic phonon energies.

A more comprehensive theory by Kulik et al. (see Section 3.2) based on the solution of the Boltzmann equation confirmed the phenomenological formula (2.6) and became the founding issue for PCS. The voltage V applied to the contact defines the energy scale eV for the scattering processes. For the nonequilibrium situation of an applied voltage across a ballistic contact, the Fermi surface splits into two parts with a difference in their maximum energy given by the bias-voltage energy eV (see Section 3.1). This energy step in the distribution of available electron states close to the contact is, figuratively speaking, the energy-resolving probe in point-contact spectroscopy.

The use of point contacts provides spectroscopy with all kinds of quasiparticle excitations in conductors. Along with the traditional investigation of

the electron– phonon interaction, other types of interactions that result in an energy-dependent relaxation time $\tau(\epsilon)$ can be studied by PCS: electron–magnon interaction, Kondo scattering, crystal-field levels of the rare-earth ions, and so on.

2.3 Superconducting contacts

Point contacts with superconductors were used for the investigation of the superconducting phenomena as well as for many applications. It is difficult to cover all aspects of superconducting contacts, but from a spectroscopic viewpoint, one mainly deals with such phenomena as the Josephson effects and Andreev reflection. For the Josephson effects in superconductor–superconductor contacts, we refer to the books by Kulik and Yanson (1970), Barone and Paterno (1982), and Likharev (1985). Here we will mostly concentrate on the Andreev reflection phenomenon for the electrical transport across a normal-metal superconductor interface. The Andreev reflection describes the process of charge transfer between single particle charge carriers in normal metals and Cooper pairs in superconductors.

An electron at the Fermi level cannot cross an interface with a superconductor because of the existence of an energy gap with forbidden quasiparticle states. In 1964, Andreev predicted that the electronic transfer across the interface involves the simultaneous reflection of a hole leaving a Cooper pair into the superconductor for the charge transport. It results in a doubling of net current through the contact between normal metal and superconductor with a resistance twice smaller compared with a contact fully in the normal state. The extra current is known as the excess current, and it is a characteristic feature of the $I-V$ curve of a contact between normal metal and superconductor. For excitation energies above the forbidden energy gap, quasiparticles are allowed in a superconductor, so that direct transport via single-particle excitations is again possible across the interface. This change in charge transfer results in nonlinear $I-V$ curves around the voltage corresponding to the gap energy. We show this in detail in Section 3.7.1 by taking into account the specific electron/hole character of the quasiparticles in a superconductor close to the energy gap. Actually, spectroscopy of the energy gap by point contacts began after the breaking work of Blonder et al. (1982) (BTK). They used energy-dependent transmission coefficients obtained from a solution of the Bogolubov equations at the boundary to calculate the current through the ballistic N-S contact. In spite of the one dimensionality of this model, their calculations perfectly describe experimental data. As seen from Fig. 2.4, one can directly observe the gap feature in the measured $\mathrm{d}V/\mathrm{d}I$ curve and in principle estimate the gap value from the voltage position of the minimum[1]

[1] A few years before Artemenko et al. (1979) noticed that at low temperatures, conductivity of diffusive S-c-N contact has maximum at $V = \Delta$.

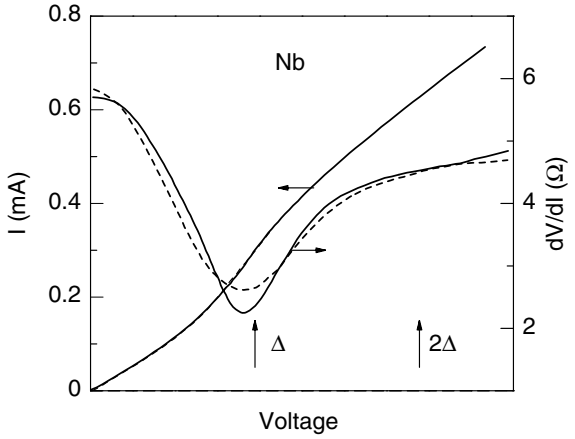

Fig. 2.4. $I - V$ curve and its derivative for a Nb-Cu point contact (solid lines) compared with the calculation by virtue of the BTK theory (dashed line) using Δ = 1.47 meV, Z = 0.65 and T/T_c = 0.138, where T_c is the critical temperature of Nb. Data taken from Blonder and Tinkham (1983).

in $\mathrm{d}V/\mathrm{d}I$ without the need of a full calculation according to the BTK theory. The latter includes also some phenomenological transmission coefficient Z of the N–S interface, which in a simple way describes a continuous transition from a metallic contact to a tunnel junction. In brief, with point contacts, it is possible to investigate the energy gap in superconductors as well as with the tunneling measurements. Over the last two decades, point contacts have been widely applied for the investigation of Δ in high-T_c materials, heavy fermion systems, borocarbides, organic and other superconductors.

2.4 Tunneling phenomena

Quantum mechanical tunneling in physics is connected with a long-time known phenomena of the emission of α-particles from radioactive nuclei, the ionization of atoms, or the cold emission of electrons in a strong electric field. In solid-state physics, tunneling is mainly connected with artificial structures that contain a potential barrier on an atomic length scale. Starting from the Esaki (1958) tunnel diode developed in 1958 and the metal-insulator-metal structure produced by Giaever (1960) a few years later, the scanning tunneling microscope initially developed in 1982 by Binning and Rohrer is nowadays transformed into a routine device with the possibility of precise control (better as 0.1Å) of the vacuum gap between the electrodes. A schematic model of the potential distribution near a tunnel junction between two conductors is shown in Fig. 2.5(a) with different transmission channels. By applying to a tunnel contact with nonzero tunneling transmission, a small bias voltage

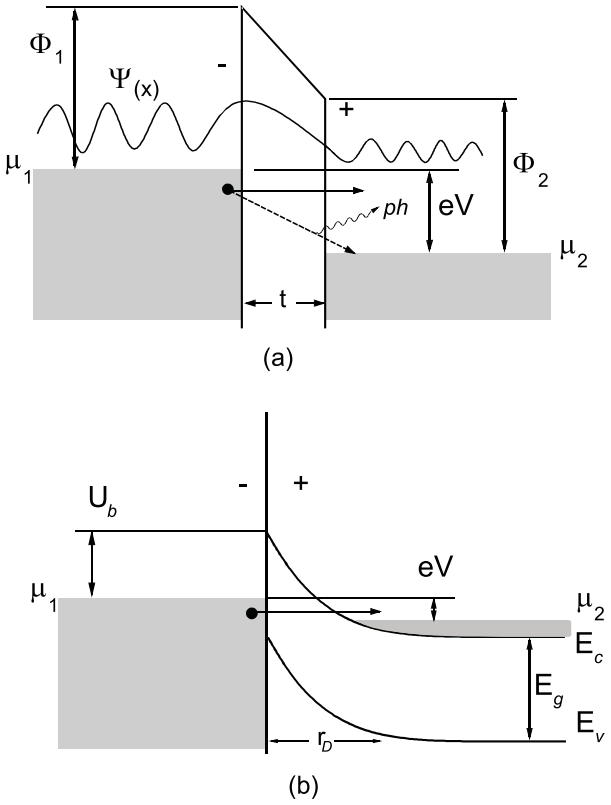

Fig. 2.5. (a) Scheme of a voltage V biased tunnel contact between two metals 1 and 2. Elastic and inelastic tunneling processes are shown by solid and dashed arrows, respectively. Ψ is the wave function, Φ is the workfunction, μ is the chemical potential, and t is the barrier width. *ph* marks excitations like phonons. (b) Scheme of voltage V biased Schottky barrier between a metal and a degenerate n-type semiconductor with a gap $E_{\rm g}$ between the bottom E_c of the conduction band and the top E_v of the valence band. $r_{\rm d}$ marks the Debye charge screening length in semiconductor, and U_b is the height of the barrier.

compared with the workfunction of the metal, the tunnel current will be proportional to the applied voltage and is defined by the junction resistance

$$R = R_0 \exp\left(\frac{2t}{\hbar}\sqrt{2\mathrm{m}\Phi}\right), \tag{2.7}$$

where R_0 is a prefactor that depends on various parameters, t is the barrier width, m is the electron mass, and Φ is the metal workfunction. This exponential dependence of the resistance on the width of dielectric gap, e. g., increase of the gap with 1Å , changes the resistance about one order of magnitude,

is used in a scanning tunnel microscope as an extremely sensitive method to measure surface corrugations with a subangström resolution.

One of the very fruitful applications of tunneling spectroscopy was the observation of the superconducting energy gap Δ by Giaever (1960). The current of a voltage-biased $S_1 I S_2$ tunnel junction depends on the quasiparticle density of states (DOS) $N_i(\epsilon)$ in the superconducting electrodes S_i $(i = 1, 2)$ such that [Wolf (1985)]

$$I(V) \propto \int_{-\infty}^{\infty} N_1(\epsilon) N_2(\epsilon + eV)(f(\epsilon) - f(\epsilon + eV))\mathrm{d}\epsilon, \tag{2.8}$$

where $f(\epsilon)$ is the Fermi–Dirac distribution function. For superconductors with a gap Δ in DOS ($N_i^{\mathrm{S}}(\epsilon) = 0$ at $e|V| \leq \Delta_i$), the tunnel current is zero for a bias voltage below $(\Delta_1 + \Delta_2)/e$ and increases to the normal-state current at higher bias voltages. In the case of SIN junction, the derivative of (2.8) with respect to the applied voltage assuming a constant density of states for the normal-metal electrode N results in

$$\mathrm{d}I/\mathrm{d}V \propto N_{\mathrm{S}}(\epsilon)$$

for $T \to 0$. Hence, the tunnel junction presents a tool for the spectroscopy of the quasiparticle density of states in superconductors, which gives direct information on the superconducting energy gap [Giaever (1960)]. Moreover, the electron–phonon interaction (EPI) modifies the DOS of the superconductor, what results in small variations of the tunnel current that can be clearly seen in the $\mathrm{d}^2I/\mathrm{d}V^2\,(V)$ curves of junctions of superconductors with a strong EPI (Fig. 2.6). As an example for Pb, Fig. 2.6 reveals distinct features in the second derivative reflecting the EPI in the metal. However, unlike in PCS, there is not a direct proportionality between $\mathrm{d}^2I/\mathrm{d}V^2\,(V)$ and the EPI function α^2F. The EPI function can be reconstructed from the experimental data by a self-consistent iteration procedure based on the solution of the Eliashberg equation for the gap function [McMillan and Rowell (1965)].

Tunnel contacts between normal metals can also be used for spectroscopy. Electrons with a well-defined excess energy up to eV may interact with the quasiparticle excitations in the electrodes and/or in the barrier as well as with the molecules absorbed at the interface of the tunnel junction [see Jaklevic and Lambe (1966)]. The energy resolved detection of these excitations, mostly vibrational modes, is known as inelastic electron tunneling spectroscopy. Therefore, the vibrational frequencies of molecules or barrier oxides, the energies of plasmons or spin waves, the Kondo scattering, and a variety of other excitations have been measured by tunneling spectroscopy [Wolf (1985)]. Here we should emphasize that tunneling spectroscopy of the inelastic scattering of electrons leads to an opposite sign of the correction to the current compared with PCS. The tunneling current correction increases the net current because inelastic scattering opens additional channels for the

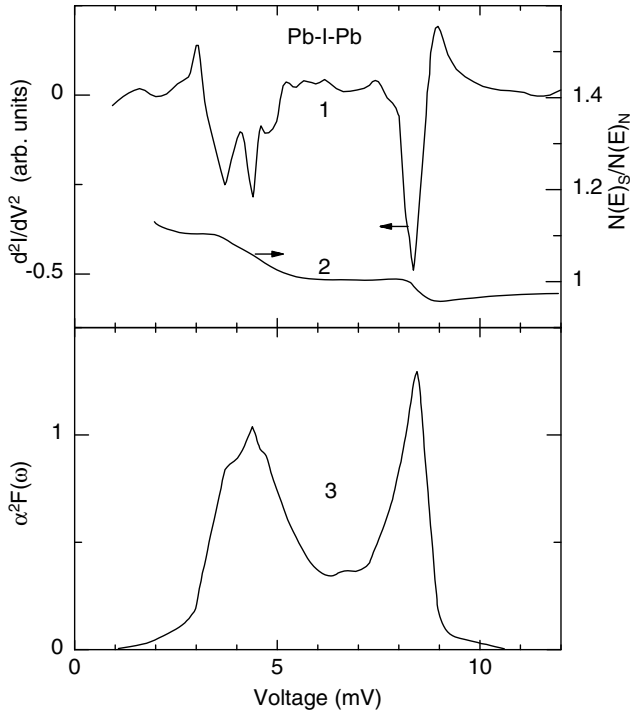

Fig. 2.6. Normalized second $\mathrm{d}^2I/\mathrm{d}V^2\,(V)$ derivative (curve 1) of Pb-I-Pb tunnel contact (I stands for insulator) with Pb in the superconducting state at 0.8 K. Curve 2 is the experimentally obtained normalized density of states in the superconducting state. Curve 3 represents the EPI function derived from the above experimental data [compare with point contact spectrum presented in Fig. 2.3 (bottom curve)]. Data taken from McMillan and Rowell (1965).

electron tunneling across the insulating barrier [see Fig. 2.5(a)]. The tunneling current depends strongly on the DOS. As we will show further, DOS effects can be neglected in a first approximation for the transport in ballistic point contacts.

Finally, we present an example of a tunnel junction known as the Schottky barrier [Fig. 2.5(b)]. This barrier originates in the contacts between a metal and a semiconductor if the difference between workfunction of metal and semiconductor is positive $\Phi_m - \Phi_s = U > 0$. One should keep in mind that this kind of barrier caused by a charge redistribution at the interface could also play a role in the investigation of metallic contacts with conductors of a low (at least on the surface) carrier concentration.

References

Artemenko S. N., Volkov A. F. and Zaitsev A. V. (1979) Solid State Communs. **30** 771.

Barone A. and Paterno G. (1982) *Physics and Applications of the Josephson Effect* Wiley-Interscience, New York.

Blonder G. E. and Tinkham M. (1983) Phys. Rev. **27** 112.

Blonder G. E., Tinkham M. and Klapwijk T. M. (1982) Phys. Rev. **25** 4515.

Esaki L. (1958) Phys. Rev. **109** 603.

Giaever I. (1960) Phys. Rev. Lett. **5** 147, ibid. 464.

Grimvall G. (1981) *The Electron–phonon Interaction in Metals* North-Holland Publ. Co., Amst., N.-Y., Oxf.

Jaklevic R. C., and Lambe J. (1966) Phys. Rev. Lett. **17** 1139.

Kulik I. O. and Yanson I. K. (1970) *The Josephson Effect in Superconductive Tunneling Structures* (Nauka, Moskow) [English trans. by Israel Program for Scientific Translation Ltd; 1972, Keter Press, Jerusalem].

Likharev K. K. (1985) *Introduction to the Dymamics of Josephson Junctions* Moscow: Nauka (in Russian).

Maxwell J. C. (1904) *A Treatise of Electricity and Magnetism* Clarendon, Oxford.

McMillan W. L. and Rowell J. M. (1965) Phys. Rev. Lett. **14** 108.

Sharvin Yu. V. (1965) Sov. Phys. - JETP **21** 655.

Tsoi V. S. (1974) JETP Lett. **19** 70.

Wolf E. L. (1985) *Principles of Electron Tunneling Spectroscopy* Oxford University Press, Inc. New York.

Yanson I. K. (1974) Sov. Phys. - JETP **39** 506.

http://www.springer.com/978-0-387-21235-7

Point-Contact Spectroscopy
Naidyuk, Y.G.; Yanson, I.K.
2005, XI, 297 p. 35 illus., Hardcover
ISBN: 978-0-387-21235-7